

Preparation of innovative metallic composite glazes for porcelainized stoneware tiles

C. Siligardi^{a,*}, L. Tagliaferri^a, L. Lusvarghi^a, G. Bolelli^a, D. Venturelli^b

^aDepartment of Engineering “Enzo Ferrari”, University of Modena and Reggio Emilia, Via Vignolese 905/a, 41125 Modena, Italy

^bColorobbia Italia, Via Bucciardi 35, Fiorano Modenese, 41042, Italy

Received 15 April 2013; received in revised form 20 May 2013; accepted 21 May 2013

Available online 20 July 2013

Abstract

Innovative metallic glazes for porcelain stoneware tiles, containing stainless steel and a special Ni-based alloy (NiCoCrAlY, commonly used as bond coating material in thermal barrier coating systems on Turbogas superalloy components), have been studied. These new products, called “metallic composite glazes” (MCGs), showed different aesthetic properties than usual lustres or metallic glazes. After heating, the surfaces of these innovative glazes did not display any interesting behaviour, but, after polishing, a particular metallic aesthetic effect has been found. These new glazes can be described as composite materials made of a glass matrix reinforced with metal particulates. A deep characterisation of metallic powders and MCGs was performed by using several techniques. The glazes containing the NiCoCrAlY powders manifested the best aesthetic, microstructural, thermal and chemical properties.

© 2013 Elsevier Ltd and Techna Group S.r.l. All rights reserved.

Keywords: A. Solid state reaction; B. Composites; C. Chemical properties; D. Traditional ceramics

1. Introduction

Metallic glazes are a new particular type of ceramic decoration able to provide surface aesthetic properties (metallic shine) as *lustres* usually do. Lustres are the ancestor of these new materials: they were manufactured using metals as copper, iron, tungsten, silver and sometimes gold, added to the composition of the frits. In literature works, they have been defined as thin, nanostructured surfaces used as decoration for ceramic glazes [1]. Lustres have been studied for a long time as they come from the ancient Arabic pottery: the ancient procedure to create lustres involved adding the metals in the form of salts or oxides, on the surfaces of the glaze, and consolidating them using a sort of “third firing” process with a reducing atmosphere [2]. In order to create a reducing atmosphere, some studies related to lustres suggested the use of carbon black as part of the glaze as reducing element [3]. In some other reported researches, the formation process of lustres consisted of ion-exchange of alkalis (Na and K) by Cu

and Ag, diffusion of the metal ions into the glaze and reduction of the metal ions to metallic nanoparticles [4]. Nowadays, the procedure to create lustres is adding metals as raw material into the frit composition in order to seal them into the glass matrix. Frits are then melted at high temperature and quickly cooled. This process causes a thermal shock to the glass, which consequently breaks up into little particles. At the end of the procedure, a frit is therefore obtained, which contains embedded metals or metal oxide particles that provide particular optical and decorative properties [5].

In some cases, the frit is then added to a mixture of other raw materials, taking part to the composition of the glaze. Unlike *lustres*, metallic glazes follow a different preparation procedure and they usually show the optical and aesthetic characteristics of the added metals. Specifically, metal powders are added to the glaze composition and not to the frit composition any more.

The present manuscript reports the production and characterisation of new metallic glazes, where the selected metal powders added to the glaze composition are stainless steel and a Ni-based superalloy belonging to the NiCoCrAlY alloys family. The main aim of the work is to design and create a new

*Corresponding author.

E-mail address: cristina.siligardi@unimore.it (C. Siligardi).

material for ceramic decoration using new types of metallic powders, selecting the most suitable kind of metals able to be added into new materials for ceramic decoration (metallic glazes). The stainless steel powders are already employed in the industry for the production of metallic composite glazes, while NiCoCrAlY powders, which have never been previously used, could provide better resistance against corrosion and degradation during high temperature firing ($> 1200\text{ }^{\circ}\text{C}$).

The characterisation has been carried out on the metallic powders and on the final glazes. The characterisation was performed by using X-Ray fluorescence (XRF), Differential Thermal Analysis (DTA) and thermogravimetry, laser size distribution analysis, X-ray diffraction (XRD), Scanning Electron Microscopy (SEM) with Energy Dispersion Spectroscopy (EDS). The chemical properties of the glaze surface were also tested.

2. Experimental procedure

The metallic powders used in this research were steel powders (AISI316L, Cogne Acciai Speciali S.p.A., Italy) and NiCoCrAlY powders, which are commonly used as raw material in the deposition process of thermal barrier coating systems as bond coating material (Turbocoating S.p.A., Italy) [6,7]. The chemical composition of the NiCoCrAlY metallic powders was investigated by X-Ray Fluorescence (XRF: Advant'X, ThermoFisher Scientific, Waltham, MA, USA). The thermal behaviour was studied by Differential Thermal Analysis (DTA) and Thermo-gravimetric (TG) Analysis (STA429, Netzsch, Selb, Germany). The mineralogical characterisation of powders was performed by X-ray Diffraction (XRD: PANalytical, PW 3710 diffractometer) and surface microstructure was investigated by Scanning Electron Microscopy (SEM: Philips XL 40) with Energy Dispersion Spectroscopy (INCA: Oxford Instrument Analytical, High Wycombe, UK). Their particle size distribution was assessed by laser diffraction technique (Mastersizer 2000, Malvern Instruments, Malvern, UK) using the wet dispersion method (Hydro-S wet dispersion unit). The glazes were prepared at the laboratory scale simulating the industrial tile manufacturing process. The first step consisted in mixing and wet grinding the raw materials (Tables 1 and 2) in porcelain jars with dense alumina grinding media for 20 min in a planetary mill. The glazes were applied onto black-pigmented-engobed green single-fired wall tiles ($300 \times 300 \times 5\text{ mm}^3$) using a silk-screen printing technique. The thickness of the final layer glaze was about $25\text{ }\mu\text{m}$. The engobe was applied on the green tile by disc application [8,9]. After glazing, the resulting tiles were dried at $120\text{ }^{\circ}\text{C}$ for

Table 2

Transparent glaze composition used to prepare metallic glaze composite.

Transparent glaze	wt%
Glass-ceramic frit	31.8
Transparent frit	16.0
Caolin	4.4
Dolomite	2.5
Corundum	5.3
Nepheline	40.0

2 h and fired in an industrial gas kiln in an oxidising atmosphere (10 vol% of oxygen) at the maximum temperature of $1200\text{ }^{\circ}\text{C}$, in a cold to cold cycle of 45 min. Subsequently, the glazed tiles were polished starting from a 400 mesh SiC abrasive paper and finished with 1800 mesh one. The glazes containing steel powders and NiCoCrAlY powders were labelled as T1 and T2, respectively. The characterisation of the glazes was performed using multiple techniques. X-ray diffraction (XRD, PANalytical, X'Pert PRO diffractometer, using Cu-K α radiation and an X'Celerator detector on the diffracted beam path) was performed on glaze specimens to detect and identify the crystalline phases formed during the heat treatments. Patterns were collected in the $10\text{--}80^{\circ} 2\theta$ range with step size of 0.02° and 3 s time/step, which are the same experimental parameters used for the XRD analysis of the powders. A scanning electron microscope (SEM, FEI XL-30) was used to observe the microstructure of the polished surfaces and cross-sections of the glazed tiles. A qualitative chemical analysis was obtained by means of an energy dispersive X-ray spectrometer coupled to the SEM. The chemical durability in HCl was tested according to the ISO 10545-13:1995 standard related to glazed tiles. The tile is held in such a manner that image of a lamp is reflected on the untreated surface. The angle of incidence of the light upon the surface shall be approximately 45° and the distance between the tile and the light source shall be $(350 \pm 100)\text{ mm}$. The criterion of judgement shall be the sharpness of the reflection and not the brightness of the surface. The tile must be positioned so that the image falls simultaneously on both treated and untreated parts and determine whether it is any less clear on the treated part. The visual inspection allows ranking the glazes in different classes: class A corresponds to no visible effect, class B to definite change in appearance, and class C to partial or complete loss of the original surface. Finally, the aesthetic properties of the coatings was examined measuring the colour Hunter parameters, L^* , a^* , b^* (X-Rite, ColorEye XTH), before and after the chemical durability test. The total colour difference and ΔE^* was also be calculated. The ΔE^* is a single value which takes into account the differences between L^* , a^* , and b^* of the tested sample and the standard, i.e. the sample before the chemical durability test. The more the measured value of ΔE^* between the tested sample and the “standard” reference exceeds the numerical range 0.5–1, the more the aesthetic properties of the untested sample can be altered by a chemical attack, losing the initial aesthetic characteristics [10].

Table 1

Raw materials composition used to prepare metallic glaze composite.

Metallic composite	Glaze composition (wt%)
Metallic powders	45.7
Copper alloy	2.4
Transparent Glaze	48.0
Bentonite	3.9

Table 3

Composition of the steel (technical data sheet) (a) and NiCoCrAlY (b) powders.

(a) Element	C	Cr	Ni	Mo	Si	Mn
(%)	0.03	17	12	2.5	0.5	1.5
(b) Element	Ni	Co	Cr	Al	Y	
(%)	31	38	22	8	1	

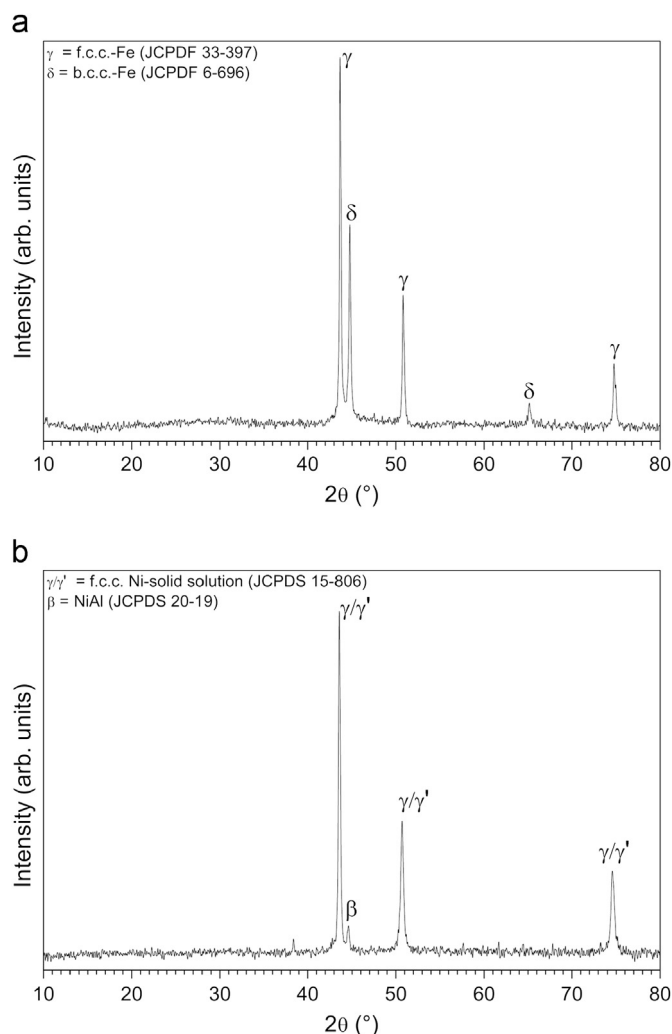


Fig. 1. XRD patterns of metallic powders: (a) steel and (b) NiCoCrAlY.

3. Results and discussion

3.1. Metal powders characterisation.

The chemical analysis of the metallic powders, obtained by the XRF technique, is shown in Table 3a and b. The chemical composition of stainless steel reveals the presence of a high percentage of iron and chromium (typical of stainless steel). Approximately 3% Mo and 8% Ni are also present, being an austenitic stainless steel. The composition of the NiCoCrAlY

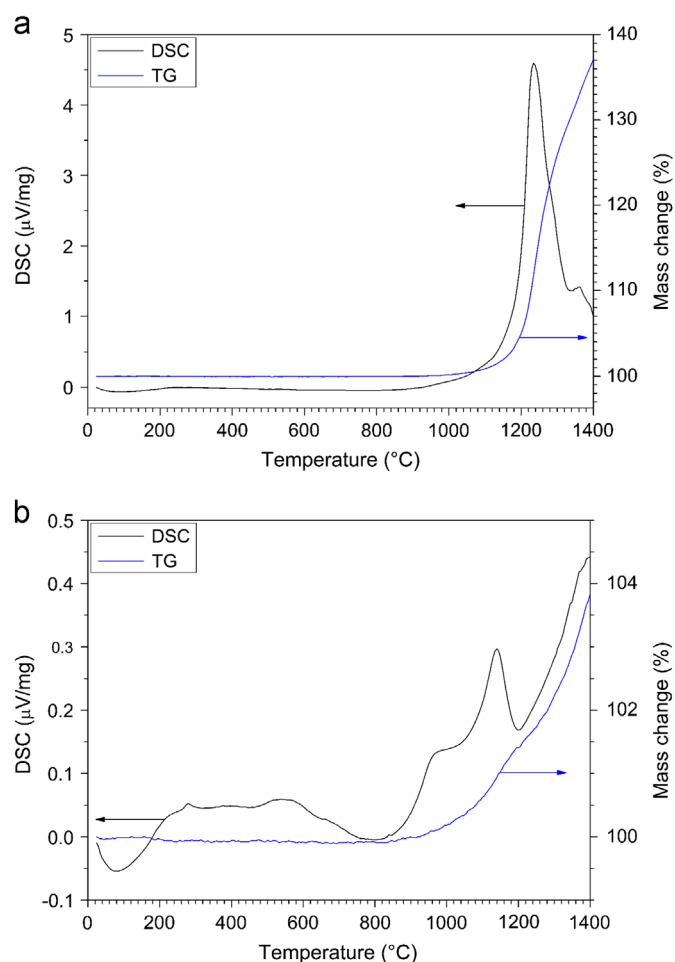


Fig. 2. DTA/TG thermograms of metallic powders: (a) steel and (b) NiCoCrAlY.

superalloy shows high percentages of Nickel, Chromium and Cobalt higher than 25%. Another important feature of this alloy is the presence of about 8% of Al: this latter element confers the peculiar oxidation resistance properties to this alloy, thanks to the high temperature formation of a thermally grown oxide (Al_2O_3 scale), which allows NiCoCrAlY coating to be used as a bond coating in the TBC systems [11].

The XRD patterns of the metallic powders are shown in Fig. 1a and b. In the steel powder, apart from the peaks of the austenite main phase (in accordance with Ref. [12]), δ -ferrite phase is also present (similarly to [12]), which is probably a consequence of rapid cooling of the alloy from the melt during powder

manufacturing by gas atomisation process. The NiCoCrAlY powder shows two main phases, the γ/γ' (JCPDS #15-0806) phase, an f.c.c. solid solution of Ni, Co and Cr, and the β -phase (JCPDS #20-0019), i.e. the NiAl intermetallic compound [13–16]. The thermal stability of the powders was measured by using a TG-DTA analysis. The thermograms were reported in Fig. 2a and b. The steel is thermally stable up to 1100 °C (TG curve); at higher temperature, its weight start increasing and around 1200 °C an intense oxidation reaction occurs (DTA curve), corresponding to a further significant increase in weight (TG curve) of 38% at 1400 °C. The oxidation phenomena are mainly due to the oxidation of chromium at lower temperatures, and, at higher ones, of iron and nickel as well, which leads to the formation of mixed oxides and spinels [17].

The thermal behaviour of the NiCoCrAlY is reported in Fig. 1b: the sample is thermally stable up to 900 °C (TG curve), when an oxidation reaction starts being active, leading to an exothermic peak at 1100 °C. This reaction is known to be due to the formation of Al- and Y-based oxides; as the temperature increases and Al is depleted from the alloy, other oxides are formed as well (e.g. Cr_2O_3 , NiO and spinel oxides) [18–20]. The weight increase at 1400 °C is anyway much lower (4%) than that for steel.

The particle size distributions of the two metallic powders (Fig. 3a and b) exhibit some differences. They both present a monomodal curve, although the steel powder shows a peak value at 106 μm , while the NiCoCrAlY one has a peak at 74 μm . This result is confirmed by the characteristic values: in fact for steel D10, D50 and D90 are respectively 65 μm ,

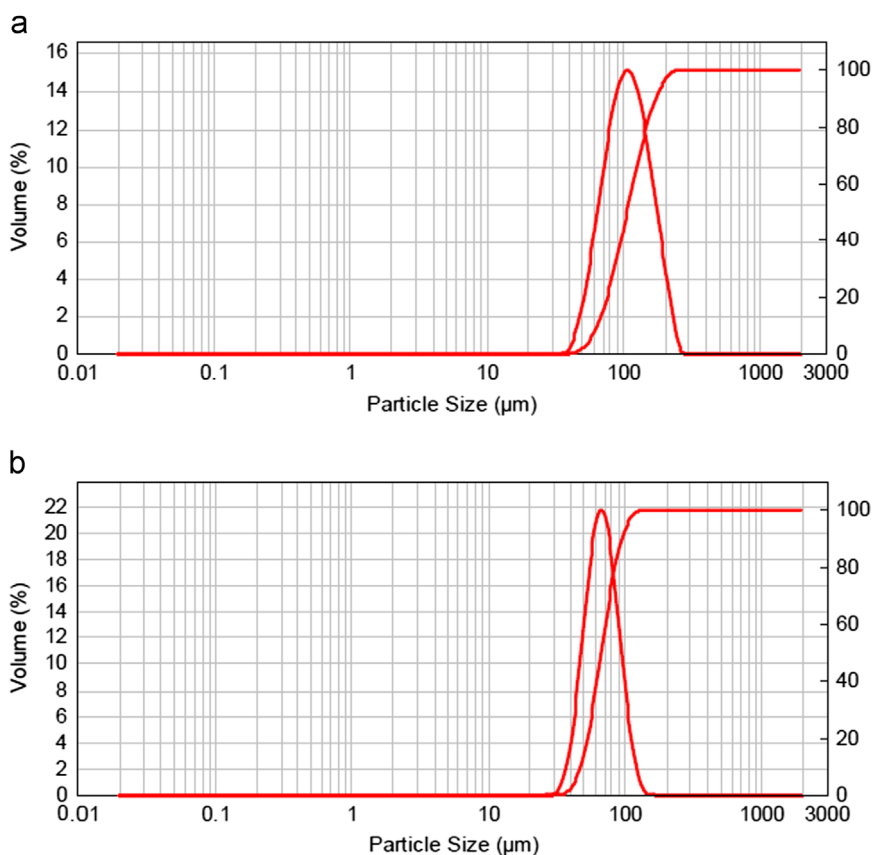


Fig. 3. Particle size distribution of metallic powders: (a) steel and (b) NiCoCrAlY.

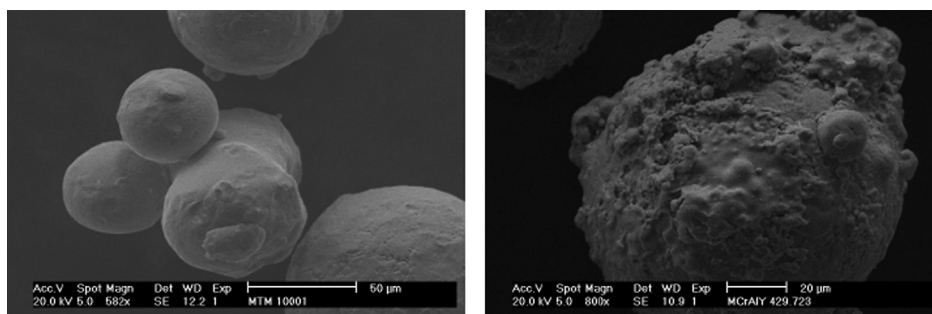


Fig. 4. SEM image of metallic powders. The figure on the right shows the morphology of the steel powders, while the figure on the left concerns NiCoCrAlY powders.

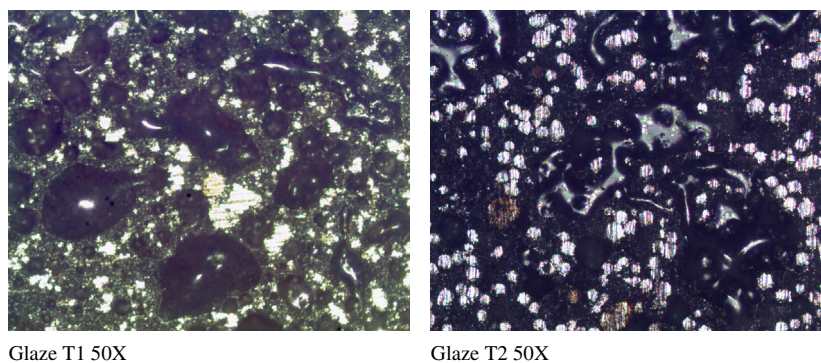


Fig. 5. Optical microscope images of polished glazes.

106 μm and 173 μm while, for NiCoCrAlY powders, they are respectively 47 μm , 67 μm and 95 μm .

The surface morphology of the powders was observed with a scanning electron microscope while a semi-quantitative chemical analysis was performed by using an energy dispersion spectroscopy.

The steel powder shows (Fig. 4a) a spherical geometry and a clean, smooth surface: this property is typical of gas-atomized powders. The NiCoCrAlY powder particles also exhibit rounded morphology, with a large number of finer particles (“satellites”) and splats attached onto their surface (Fig. 4b), which is also typical of a gas atomising process [21]. Depending on the operating conditions, indeed, some of the finer liquid metal drops can stick onto the surface of larger particles, thus making them rougher and more irregular.

3.2. Metallic glazes composites characterisation

The glazed tiles, after the firing process, presented a dark colour, a matt appearance and a rough surface. The aesthetical properties of these surfaces are quite poor. After polishing, the glaze surfaces changed completely and showed interesting aesthetic peculiarities. The macrostructure of the surface was investigated using an optical microscope (Fig. 5). Fig. 5 shows some metallic particles (light zone) immersed into a dark glassy matrix. Some porosity is also present in the T1 glaze, due to the polishing process that removed some metallic particles from the glaze (see SEM results). SEM+EDS microanalysis was also performed to obtain further details of the surface microstructures before and after polishing and on the cross-section (Fig. 6). The unpolished surfaces show quite similar microstructure (Fig. 6a and b). The surfaces are quite rough due to the presence of metal particles immersed in a glassy matrix. The glaze T2 shows a finer microstructure than the T1 glaze since the NiCoCrAlY metallic particles are finer than the steel ones. The polished T1 glaze (Fig. 6c) presents high open porosity: the mechanical action of polishing pulled out most of the steel particles (Fig. 6e) and, moreover, cracks can be detected around some of the steel particles in the glass matrix (Fig. 6g). Both these two features were caused by the poor adhesion between matrix (glass) and reinforcement (steel). In fact, a limited adhesion is typically present in those cases where “spalling” is detected. Spalling

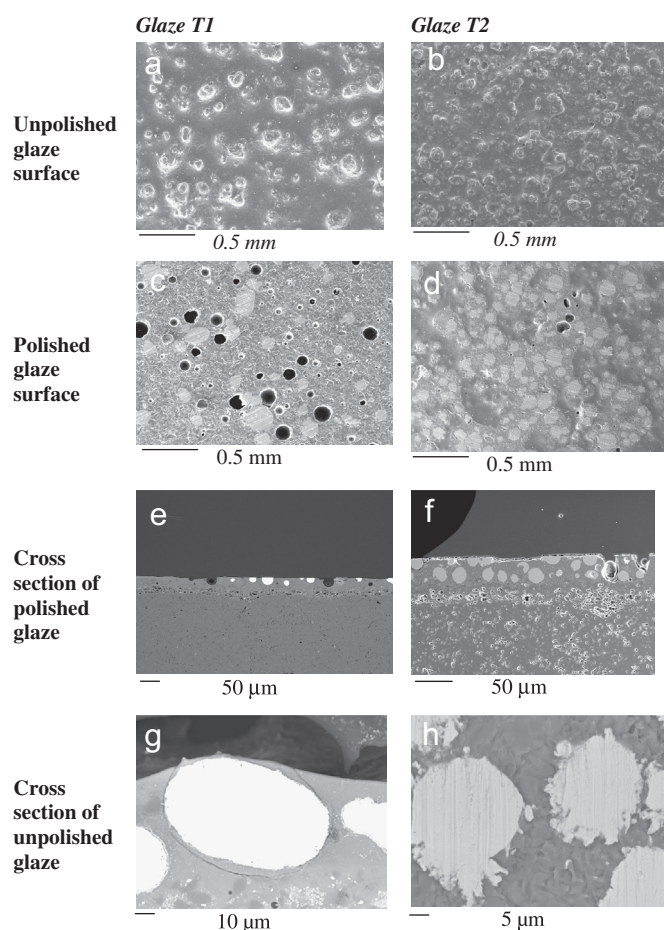


Fig. 6. Glaze T1 (a) unpolished surface, (c) polished surface, (e) cross-section polished, and (g) cross-section unpolished; glaze T2, (b) unpolished surface, (d) polished surface, (f) cross-section polished, and (h) cross-section unpolished.

occurs when two contiguous materials subjected to heating processes have quite different linear thermal expansion coefficients (α) and the adhesion at the materials interface cannot compensate the stresses induced in the cooling step of the firing process. In fact, in the temperature range from 20 to 500 $^{\circ}\text{C}$, steel possesses $\alpha \approx 18 \times 10^{-6}/^{\circ}\text{C}$, while, commonly, tile glazes possess $\alpha \approx 7\text{--}8 \times 10^{-6}/^{\circ}\text{C}$.

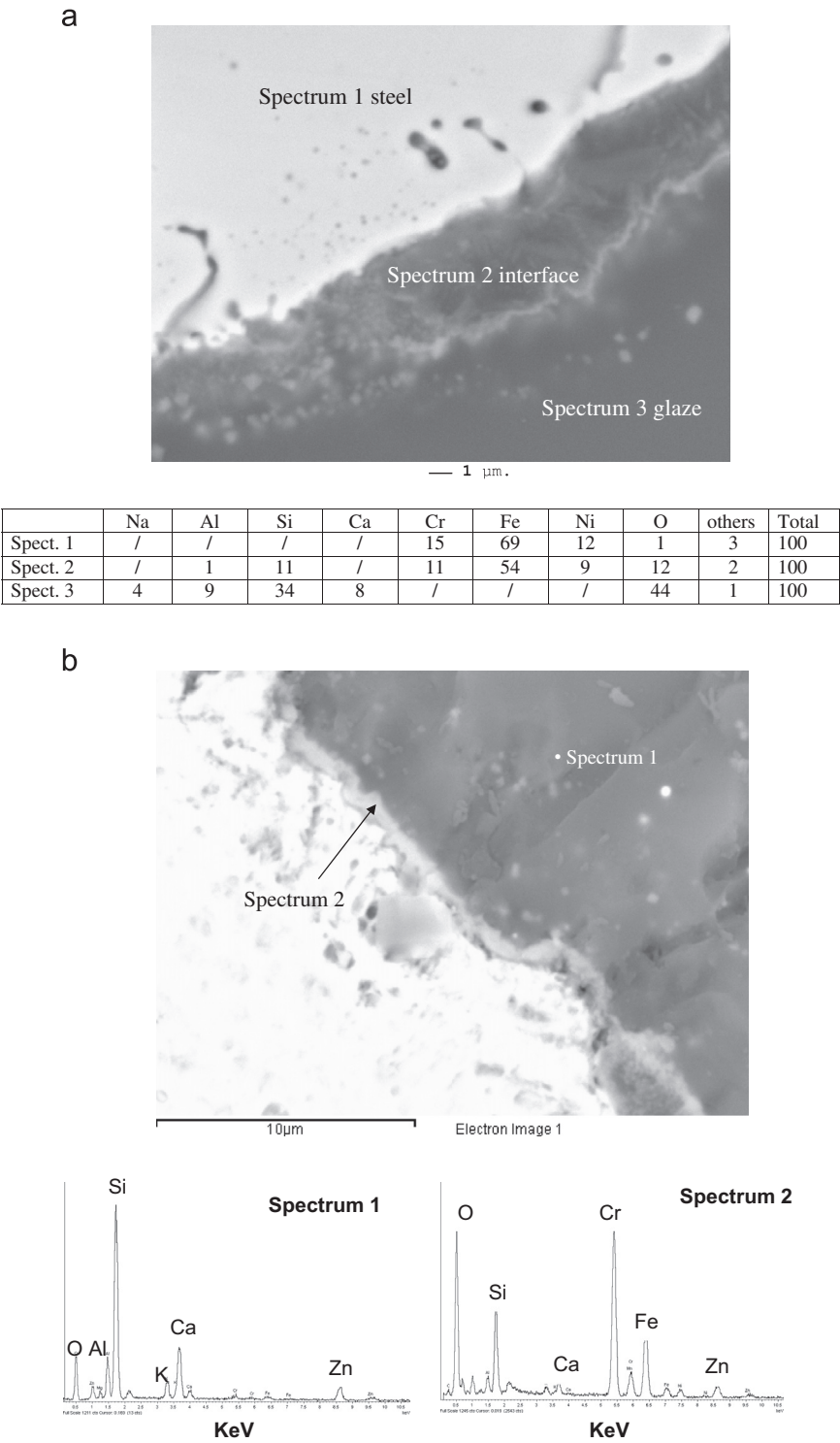


Fig. 7. SEM image and EDS spectra (wt%) of T1 glaze: (a) before and (b) after chemical treatment. The vertical axis represents the number of counts.

Concerning the glaze T2, its polished surface presents very low porosity (Fig. 6d) with respect to the T1 surface; NiCoCrAlY particles are well embedded and tightly adherent to the vitreous phase (Fig. 6f and h) and its thermal expansion coefficient is $\approx 14\text{--}15 \times 10^{-6}/^{\circ}\text{C}$ from room temperature up to $\approx 600^{\circ}\text{C}$ [19,22–24], inducing lower residual thermal stresses.

The chemical durability of the glaze surface was tested by using hydrochloric acid (HCl 3%) according to ISO 10545/13.

Fig. 7a shows the glaze T1 before chemical durability test. An interaction area at the steel–glaze interface is recognisable, where Cr ion is diffused out of the steel particle into the surrounding glass during the firing process. This is recognisable from the brighter areas (back scattered electrons chemical contrast) of the glass at the interface region, which suggests the presence of heavier elements. The latter hypothesis is confirmed by EDS spectrum, as shown in Fig. 7a.

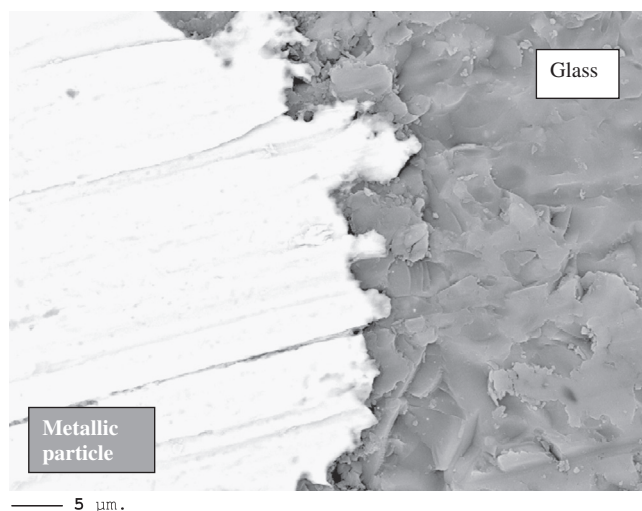


Fig. 8. SEM image of T2 glaze.

Table 4
Hunter's parameter before and after chemical test (± 0.1).

Colouring parameter	T1 before test	T1 after test	T2 before test	T2 after test
L*	29.3	30.5	32.1	32.0
a*	1.1	0.9	1.0	0.9
b*	1.2	0.3	1.8	0.7
ΔE^*		1.5		1.1

After chemical durability test, selective attack occurred in this mentioned area as demonstrated in Fig. 7b. The interface zone shows alterations of the microstructural and chemical composition (see EDS spectra). Such finding matches well with the previous observations on the microstructural features of the glaze: the acid has likely infiltrated into those cracks, which were created after the firing process, and this attack caused a variation of the chemical composition of the interface. The chemical alteration of interface after firing as reported in Fig. 7a also lowered the acid resistance of the glass in this area. In Fig. 8, an image of the T2 glaze is shown: no change to the metal–glass interface is evident. This was due to the high chemical durability of NiCoCrAlY, which prevented significant alteration of the chemical compositions at the interface. Such microstructural features have been confirmed by the outcomes of the ISO 10545-13:1995 standard test: metallic glazes T1 containing stainless steel had to be ranked as class C, while metallic glazes T2 embedding NiCoCrAlY powder could be ranked as class A.

Finally, regarding the colour parameters L^* , a^* , and b^* reported in Table 4, it is possible to note that for both glazes T1 and T2 before chemical test, the values are quite similar. After chemical test T1 sample shows a higher L^* and lower b^* values while for T2 sample, only b^* value, slightly decreases. It is important to observe that ΔE^* value for sample T1 is higher than one while for T2 is near one, allowing to conclude that the mentioned chemical alteration caused by HCl test

affected negatively also the aesthetic quality of stainless steel metallic glaze.

4. Conclusions

Different types of “Metallic glazes” have been studied. These new materials showed different properties according to the metallic powders added to the glaze composition.

The metallic glaze containing stainless steel showed bad adhesion between the glass matrix and the metal particles. In fact, cracks along the interface between the glaze and the stainless steel particles were detected: this feature caused a loss of metal particles after polishing (pull-out of the metallic particles). The NiCoCrAlY metallic glaze did not show cracks or flaws at the interface between particles and glass matrix, likely thanks to a lower mismatch between the thermal expansion coefficient of the two materials. In terms of chemical resistance, too, the glaze embedding NiCoCrAlY behaved better, showing a limited damage, thanks also to a very limited interaction of the metallic particles with the surrounding glass matrix. Consequently, quite unaltered aesthetical properties after the chemical durability test of NiCoCrAlY glaze were also found.

These new materials for ceramic decoration should be called “metallic composite glazes”, as they display similar properties to composite materials, having a glass matrix reinforced with metallic particles.

Acknowledgements

The authors gratefully thank Colorobbia Italia S.p.A (manufacturing site of Via Cameazzo, 45, 41042 Fiorano Modenese, Italy) for their help in the preparation of the samples and laboratory testing. A special thank is dedicated to Dr. Andrea Scrivani, Turbocoating S.p.A (Via Mistrali 7, 43040 Rubbiano di Solignano, Italy) and Dr. Carlo Giolli, previously employed at Turbocoating S.p.A., for having supplied the NiCoCrAlY powders and provided precious suggestions.

References

- [1] J. Roque, J. Molera, P. Sciau, E. Pantos, A. Vendrell-Saz, Copper and silver nanocrystals in lustre lead glazes: development and optical properties, *Journal of the European Ceramic Society* 26 (16) (2006) 3813–3824.
- [2] I. Borgia, B. Brunetti, I. Mariani, A. Sgamellotti, F. Cariati, P. Fermo, M. Mellini, C. Viti, G. Padeletti, Heterogeneous distribution of metal nanocrystals in glazes of historical pottery, *Applied Surface Science* 185 (3–4) (2002) 206–221.
- [3] José S. Moya, C.P. Isabel Montero, Raúl Pina-Zapardiel, Antonio Esteban-Cubillo, Julián J. Reinoso, José F. Fernandez, Fabrication of nanostructured metallized glazes by conventional fast-firing route, *Journal of the American Ceramic Society* 94 (7) (2011) 2067–2207.
- [4] J. Roque, T. Pradell, J. Molera, M. Vendrell-Saz, Evidence of nucleation and growth of metal Cu and Ag nanoparticles in lustre: AFM surface characterization, *Journal of Non-Crystalline Solids* 351 (6–7) (2005) 568–575.
- [5] C. Siligardi, M. Montecchi, M. Montorsi, L. Pasquali, Lead free Cu-containing frit for modern metallic glaze, *Journal of the American Ceramic Society* 92 (11) (2009) 2784–2790.

- [6] L. Zhao, M. Parco, E. Lugscheider, High velocity oxy-fuel thermal spraying of a NiCoCrAlY alloy, *Surface and Coatings Technology* 114 (1999) 181–186.
- [7] K.A. Khor, C.T. Chia, Y.W. Gu, F.Y.C. Boey, High temperature damping behavior of plasma sprayed NiCoCrAlY coatings, *Journal of Thermal Spray Technology* 11 (3) (2002) 359–364.
- [8] D.F. Zvezdin, A.V. Kir'yanov, Wet expansion of double-fired ceramic-tile engobes, *Glass and Ceramics* 63 (9–10) (2006) 315–316.
- [9] Various Authors, Glazing and decoration of ceramic tiles, Sala Ed., Modena, Italy, 2000, pp. 74–80.
- [10] Società Ceramica Italiana, Colour, pigments and colouring in ceramics, Sala Ed., Modena, Italy, 2003, pp. 27–38.
- [11] Z.L. Dong, K.A. Khor, Y.W. Gu, Microstructure formation in plasma-sprayed functionally graded NiCoCrAlY/yttria-stabilized zirconia coatings, *Surface and Coatings Technology* 114 (2–3) (1999) 181–186.
- [12] C. Borchers, T. Schmidt, F.G. Ärtner, H. Kreye, High strain rate deformation microstructures of stainless steel 316L by cold spraying and explosive powder compaction, *Applied Physics A* 90 (2008) 517–526.
- [13] T.A. Taylor, P.N. Walsh, Dilatometer studies of NiCrAlY coatings, *Surface and Coating Technology* 188–189 (2004) 41–48.
- [14] W.Z. Li, Q.M. Wang, Z.B. Bao, Y. Yao, J. Gong, C. Sun, X. Jiang, Microstructural evolution of the NiCrAlY/CrON duplex coating system and its influence on mechanical properties, *Materials Science and Engineering A* 498 (2008) 487–494.
- [15] P. Poza, P.S. Grant, Microstructure evolution of vacuum plasma sprayed CoNiCrAlY coatings after heat treatment and isothermal oxidation, *Surface and Coating Technology* 201 (2006) 2887–2896.
- [16] D. Mercier, C. Kaplin, G. Goodall, G. Kim, M. Brochu, Parameters influencing the oxidation behavior of cryomilled CoNiCrAlY, *Surface and Coating Technology* 205 (2010) 2546–2553.
- [17] J.C. Langevoort, T. Fransen, P.J. Geilings, On the influence of cold work on the oxidation behavior of some austenitic stainless steels: High temperature oxidation, *Oxidation of Metals* 21 (5–6) (1984) 271–284.
- [18] M. Seraffon, N.J. Simms, J. Sumner, J.R. Nicholls, The development of new bond coat compositions for thermal barrier coating systems operating under industrial gas turbine conditions, *Surface and Coating Technology* 206 (2011) 1529–1537.
- [19] J.J. Liang, H. Wei, Y.L. Zhu, X.F. Sun, Z.Q. Hu, M.S. Dargusch, X.D. Yao, Influence of Re on the Properties of a NiCoCrAlY Coating Alloy, *Journal of Material Science and technology* 27 (5) (2011) 408–414.
- [20] G.J. Yang, X.D. Xiang, L.K. Xing, D.J. Li, C.J. Li, C.X. Li, Isothermal oxidation behavior of NiCoCrAlTaY coating deposited by high velocity air-fuel spraying, *Journal of Thermal Spray Technology* 21 (3–4) (2012) 391–399.
- [21] S. Özbilen, Satellite formation mechanism in gas atomized powders, *Powder Metallurgy* 42 (1) (1999) 70–78.
- [22] T. Taylor, J. Foster, Thermal expansion of Tribomet MCrAlY coatings, *Surface and Coating Technology* 201 (2006) 3819–3823.
- [23] J.J. Liang, H. Wie, Y.L. Zhu, X.F. Sun, Z.Q. Hu, M.S. Dargusch, X. Yao, Phase constituents and thermal expansion behavior of a NiCrAlYRe coating alloy, *Journal of Material Science* 46 (2011) 500–508.
- [24] T.A. Taylor, P.N. Walsh, Thermal expansion of MCrAlY alloys, *Surface and Coating Technology* 177–178 (2004) 24–31.